

Energy Levels, Transition Probabilities and Electron-Impact Excitations Of Ge-Like Pr, Nd, Pm, Sm and Eu ions

O. Nagy and Fatma El_Sayed*

Physics Department, Faculty of Science, Kafrelsheikh University, Egypt

Abstract

Energies, wavelengths, transition probabilities, and oscillator strengths have been calculated for the $4s^2 4p^2 \rightarrow 4s4p^3$, $4s^2 4p^2 \rightarrow 4s^2 4p4d$ and $4s4p^3 \rightarrow 4p^4$ allowed transitions in heavy Ge-like ions with $Z=59-63$. The fully relativistic Multiconfiguration Dirac-Fock (MCDF) method taking into account both the correlations within the $n=4$ complex and the quantum electrodynamic (QED) effects have been used in the calculations. MCDFGME code is used to calculate electron impact excitation cross sections for the $4s^2 4p^2 \rightarrow 4s4p^3$, and $4s^2 4p^2 \rightarrow 4s^2 4p4d$ transitions with plane-wave Born approximation. The results of **Pr XXVIII**, **Nd XXIX**, **Pm XXX**, **Sm XXXI** and **Eu XXXII** are compared with HFR method results.

Contents

1. Introduction	2
2. Calculations	3
3. Results and Discussion	3
3.1 Energy Levels	3
3.2 Wavelengths, Transition Probabilities and Oscillator Strengths	4
3.3 Collision Strengths and Cross Sections for Electron-Impact Excitation	4
4. Conclusions	5
Acknowledgement	6
References	6

1. Introduction

Atomic collision processes are important in many fundamental and applied areas of current research [1]. The modeling and diagnostics of astrophysical and laboratory

✉ fatmamahrous@sci.kfs.edu.eg

plasmas depend on accurate atomic data for the collision strengths and cross sections of the various collision processes that might occur in them. The data required involves mainly electron-ion collisions, and includes excitation, recombination (radiative and dielectronic), and ionization processes. The most important indirect ionization process is excitation-autoionization.

Electron impact excitation cross section of highly ionized ions are needed in developing lasers in extreme ultraviolet (EUV) and soft X-ray regimes, in astrophysics and in the study of inertial confinement fusion and other laboratory-produced plasmas.

Recently, extreme ultraviolet (EUV) light sources for microlithography are receiving much attention as an application of laser-produced high-Z plasmas where the 13.5 nm light source produced in tin plasmas was thought to be attractive due to its compactness and high emissivity [2]. Theoretical analysis of the opacity and the emissivity in both EUV light sources and X-ray lasers is important to design and optimize the laser produced high-Z plasmas. Therefore, the needs for atomic data for those high-Z elements are urgent. The most successful method to produce saturated X-ray laser output is a scheme where the collisional excitation is one of the dominant atomic processes in these plasmas.

Accurate electron-impact excitation cross sections are needed for proper interpretation of the spectral emission of highly charged ions and utilizing spectral measurements for plasma diagnostics [3]. The determination of the ionization balance for a given plasma temperature is especially sensitive to the values of the excitation cross sections used to correlate the intensity of a given line to the abundance of the corresponding ion species.

Knowing the correct charge state distribution is critical for understanding radiation levels, energy deposition and energy balance of high temperature plasmas.

In this study, energy levels, radiative rates and electron impact excitation for fine-structure levels of Pr^{27+} , Nd^{28+} , Pm^{29+} , Sm^{30+} and Eu^{31+} ions are calculated using mcfgme [4] code (**M**ulti-**C**onfiguration **D**irac-**F**ock and **G**eneral **M**atrix **E**lements).

2. Calculations

The wavelengths, transition probabilities and oscillator strengths for the $4s^2 4p^2 \rightarrow 4s 4p^3$, $4s^2 4p^2 \rightarrow 4s^2 4p 4d$ and $4s 4p^3 \rightarrow 4p^4$ allowed electric dipole transitions were calculated for ions belonging to Ge- isoelectronic sequence. These calculations are performed using the fully relativistic MCDF approach with the *mcdfgme* program.

The orthogonality of the wavefunctions was consistently included in the differential equations by using off-diagonal Lagrange multipliers. Most of the odd and even configurations within the $n=4$ Layzer complex are included in the calculations. These configurations are $4s^2 4p^2$, $4s^2 4d^2$, $4s^2 4p 4f$, $4s^2 4f^2$, $4s 4p^2 4d$, $4s 4p 4d 4f$, $4p^4$, $4p^2 4d^2$, $4p^2 4f^2$ and $4s^2 4p 4d$, $4s^2 4d 4f$, $4s 4p^3$, $4s 4p^2 4f$, $4s 4p 4d^2$, $4s 4p 4f^2$, $4s 4d^2 4f$, $4p^3 4d$, $4p^2 4d 4f$, $4p 4d^3$ for the even and odd parities, respectively. There are some configurations like $4s 4d^3$, $4d^2 4f^2$, $4d^4$, $4p^3 4f$, $4f^4$, $4p 4f^3$, $4d^3 4f$, $4d 4f^3$, and $4s 4f^3$ have not been included in calculations because they are located high in energy. The high energy difference between configurations gives normally small contribution. The participations from the configurations with $n=5$ are so weak that to be cancelled, about 0.03%, thus these interactions are not included in our calculations.

The MCDF calculations were completed with the inclusion of the relativistic two-body Breit interaction and the quantum electrodynamic corrections (QED) which arise due to self-energy and vacuum polarization.

The HFR code [5, 6, 7] used in an ab-initio way for **Pr XXVIII**, **Nd XXIX**, **Pm XXX**, **Sm XXXI** and **Eu XXXII** ions, because of the lack of experimental data of these ions.

3. Results and Discussion

3.1 Energy Levels

The energy level values obtained using the MCDF and HFR method for the $4s^2 4p^2$, $4s 4p^3$, $4s^2 4p 4d$ and $4p^4$ configurations in heavy Ge-like ions with ($59 \leq Z \leq 63$) are presented in tables (1- 5). The main components of the computed eigenvectors in both the jj -coupling and the LS -coupling schemes are also given in these tables. In the notations, the superscript “*” corresponds to the case $j^* = l - 1/2$ while no superscript is given for $j = l + 1/2$.

Tables 1-5 show that the agreement between MCDF and HFR energy levels is within 1% in Ge-like ions.

For heavy atoms and highly charged ions, the jj -coupling is realized because the electrostatic interaction is directly proportional with Z value while the spin-orbit interaction increases as Z^4 [8].

3.2 Wavelengths, Transition Probabilities and Oscillator Strengths

The wavelengths, transition probabilities and oscillator strengths for the $4s^2 4p^2 \rightarrow 4s 4p^3$, $4s^2 4p^2 \rightarrow 4s^2 4p 4d$ and $4s 4p^3 \rightarrow 4p^4$ allowed transitions were calculated using the fully relativistic MCDF method are reported in tables (6- 10). The calculated MCDF transition probabilities are presented in both gauges- length and – velocity, while the oscillator strengths are only shown in length gauge. The agreement between the length and velocity forms of the oscillator strengths is within 10-20% for all the strong transitions (i.e. for $f \geq 0.10$) in Ge-like ions are presented. Exceptions to this are some few transitions; where the agreement is within $\approx 40\%$. Not only is this overall good agreement highly satisfactory, but it also gives a clear indication of the accuracy of the results. We present in table (11) a comparison between the MCDF, and HFR transition probabilities (in sec^{-1}) and oscillator strengths.

3.3 Collision Strengths and Cross Sections for Electron-Impact Excitation

Excitation rate coefficients (in $\text{cm}^3 \text{ sec}^{-1}$) for a transition from $i \rightarrow j$ are calculated using the following formula [9]

$$C(T) = \frac{8.629 \times 10^{-6}}{g_i \sqrt{k T_e}} \exp\left(\frac{-\Delta E_{ij}}{k T_e}\right) \gamma(T) \quad (1)$$

where γ is the effective collision strength, T_e is the electron temperature in eV, g_i is the statistical weight of the level i , ΔE_{ij} is the excitation energy, and k is the Boltzmann constant. Using a Maxwellian velocity distribution, the effective collision strengths can be defined as a function of electron temperature.

$$\gamma(i \rightarrow j) = \int_0^\infty \Omega_{i \rightarrow j} \exp\left(-\frac{E}{k T_e}\right) d\left(\frac{E}{k T_e}\right) \quad (2)$$

where E is the scattered electron energy, and $\Omega_{i \rightarrow j}$ is the collision strength. The unit of temperature is Kelvin.

The cross section $\sigma(i, j)$ for the transition $i \rightarrow j$ is expressed in terms of the collision strength $\Omega(i, j)$ as follows:

$$\sigma(i, j) = \frac{\Omega(i, j)}{\omega k_i^2} (\pi a_o^2) \quad (3)$$

where the subscripts i and j refer to the initial and final states, a_o is the Bohr radius ($\pi a_o^2 = 8.797 \times 10^{-17} \text{ cm}^2$), $\omega = (2S_i + 1)(2L_i + 1)$ and k_i^2 is the energy of the incident electron in Rydbergs (1 Ryd = 13.6057 eV).

The standard form of a Plane-Wave Born excitation cross section is

$$\sigma_{PWB} = \frac{4\pi a_0^2 R}{T} \Omega_{PWB}(T) \quad (4)$$

Where Ω_{PWB} is the collision strength and R is the Rydberg energy.

The electron impact collision strengths for the $4s^2 4p^2 \rightarrow 4s 4p^3$ and $4s^2 4p^2 \rightarrow 4s^2 4p 4d$ allowed transitions have been calculated at nine scattered electron energies ranging from 200 to 10000 eV. Tables 12- 16 list the collision strengths at different scattered electron energies.

Figures 1- 5 show the behavior of cross section (m^2) with the incident energy (eV) for $4s^2 4p^{*2} (J=0) \rightarrow 4s^2 4p^* 4d^* (J=1)$, $4s^2 4p^* 4p (J=1) \rightarrow 4s^2 4p 4d^* (J=0)$, $4s^2 4p^2 (J=0) \rightarrow 4s 4p^3 (J=1)$, $4s^2 4p^* 4p (J=2) \rightarrow 4s^2 4p 4d^* (J=3)$ and $4s^2 4p^2 (J=2) \rightarrow 4s^2 4p 4d (J=3)$ transitions in Ge-like ions $59 \leq Z \leq 63$. It is shown that the cross section shapes at the threshold and starts with a finite value for the excitation of ions.

4. Conclusions

In conclusion, we report energy levels, radiative rates and collision strengths for allowed transitions with the fully relativistic multiconfiguration Dirac-Fock method.

The accuracy of the collision strengths presented in this paper is difficult to assess due to the paucity of data available for comparison. However, since the present calculation (a) uses extensive configuration-interaction wavefunctions, (b) includes correlation terms in the total wavefunction, and (c) include the relativistic two-body Breit interaction and the quantum electrodynamic corrections (QED). It is expected that the

collision strengths are accurate to approximately 20-30%. The cross section data should be a useful reference in the development of X-ray lasers and other related fields involving highly stripped ions.

Acknowledgment

The authors wish to thank Dr. J. P. Desclaux and Dr. P. Indelicato for allowing us to use the mcdfgme code.

References

- [1] R. E. H. Clark and D. H. Reiter, "Nuclear Fusion Research, understanding Plasma-Surface Interactions", (Springer-Verlag Berlin, Heidelberg, 2005).
- [2] [S. Fujioka, H. Nishimura, K. Nishihara, A. Sasaki, A. Sunahara, T. Okuno, N. Ueda, T. Ando, Y. Tao, Y. Shimada, K. Hashimoto, M. Yamaura, K. Shigemori, M. Nakai, K. Nagai, T. Norimatsu, T. Nishikawa, N. Miyanaga, Y. Izawa, and K. Mima](#), Phys. Rev. Lett **95**, 235004 (2005).
- [3] M. J. May, P. Beiersdorfer, N. Jordan, J. H. Scofield, K. J. Reed, S. B. Hansen, K. B. Fournier, M. F. Gu, G. V. Brown, F. S. Porter, R. Kelley, C. A. Kilbourne and K. R. Boyce, Nuclear Instruments and Methods in Physics Research B **235**, 231-234 (2005).
- [4] J. P. Desclaux and P. Indelicato , *MCDFGME*, <http://dirac.spectro.jussieu.fr/mcdf>.
- [5] R. D. Cowan, "The Theory of Atomic Structure and Spectra", (Berkeley, University of California Press, 1981).
- [6] <Http://das101.isan.troitsk.ru/>.
- [7] R. D. Cowan, J. Opt. Soc. Am **58**, 808 (1968).
- [8] H. F. Beyer and V. P. Shevelko, "Introduction to the Physics of Highly Charged Ions", (IOP Publishing Ltd. 2003).
- [9] Y. Hahn, A. K. Pradhan, H. Tawara, and H. L. Zhang, "Photon and Electron Interactions with Atoms, Molecules and Ions", (Springer-Verlag Berlin Heidelberg, Germany, 2001).

Table (1): **MCDF** and **HFR** energy levels (in cm^{-1}) of $4s^24p^2$, $4s4p^3$, $4s^24p4d$, and $4p^4$ configurations for **Pr XXVIII** ion.

	JJ-coupling	J	LS	MCDF (cm^{-1})	HFR (cm^{-1})
1	$4s^2 4p^{*2}$	0	${}^3P_0^e$	0	0
2	$4s^2 4p^* 4p$	1	${}^3P_1^e$	200201	202316
3	$4s^2 4p^* 4p$	2	${}^1D_2^e$	224962	224270
4	$4s^2 4p^2$	2	${}^3P_2^e$	443435	443008
5	$4s^2 4p^2$	0	${}^1S_0^e$	491235	491593
6	$4s 4p^{*2} 4p$	2	${}^5S_2^o$	681165	691953
7	$4s 4p^{*2} 4p$	1	${}^3D_1^o$	778476	779413
8	$4s 4p^2 4p^*$	2	${}^3D_2^o$	880789	888636
9	$4s 4p^2 4p^*$	3	${}^3D_3^o$	935926	936713
10	$4s 4p^2 4p^*$	0	${}^3P_0^o$	972431	971481
11	$4s 4p^2 4p^*$	1	${}^3P_1^o$	996114	997903
12	$4s 4p^2 4p^*$	2	${}^1D_2^o$	1019895	1020722
13	$4s 4p^2 4p^*$	1	${}^3S_1^o$	1029589	1030987
14	$4s^2 4p^* 4d^*$	2	${}^3F_2^o$	1031939	1038144
15	$4s^2 4p^* 4d^*$	1	${}^3D_1^o$	1111392	1113271
16	$4s^2 4p^* 4d$	3	${}^3F_3^o$	1121390	1123447
17	$4s^2 4p^* 4d$	2	${}^3D_2^o$	1125434	1125949
18	$4s 4p^3$	2	${}^3P_2^o$	1192041	1191338
19	$4s 4p^3$	1	${}^1P_1^o$	1270737	1271832
20	$4s^2 4p 4d^*$	2	${}^1D_2^o$	1292717	1295382
21	$4s^2 4p 4d$	4	${}^3F_4^o$	1301159	1308274
22	$4s^2 4p 4d^*$	0	${}^3P_0^o$	1312852	1313313
23	$4s^2 4p 4d^*$	1	${}^3P_1^o$	1316876	1319065
24	$4s^2 4p 4d^*$	3	${}^3D_3^o$	1322933	1321375
25	$4s^2 4p 4d$	2	${}^3P_2^o$	1347102	1347380
26	$4s^2 4p 4d$	3	${}^1F_3^o$	1411411	1411173
27	$4s^2 4p 4d$	1	${}^1P_1^o$	1417679	1417722
28	$4p^{*2} 4p^2$	2	${}^3P_2^e$	1537430	1547016
29	$4p^{*2} 4p^2$	0	${}^1S_0^e$	1584081	1590566
30	$4p^* 4p^3$	1	${}^3P_1^e$	1750619	1763967
31	$4p^* 4p^3$	2	${}^1D_2^e$	1780873	1788252
32	$4p^4$	0	${}^3P_0^e$	2014312	2024246

Table (2): **MCDF** and **HFR** energy levels (in cm^{-1}) of $4s^24p^2$, $4s4p^3$, $4s^24p4d$, and $4p^4$ configurations for **Nd XXIX** ion.

	JJ-coupling	J	LS	MCDF (cm^{-1})	HFR (cm^{-1})
1	$4s^2 4p^{*2}$	0	${}^3P_0^e$	0	0
2	$4s^2 4p^* 4p$	1	${}^3P_1^e$	221615	224505
3	$4s^2 4p^* 4p$	2	${}^1D_2^e$	247172	247124
4	$4s^2 4p^2$	2	${}^3P_2^e$	487606	488526
5	$4s^2 4p^2$	0	${}^1S_0^e$	536537	538250
6	$4s 4p^{*2} 4p$	2	${}^5S_2^o$	721822	732828
7	$4s 4p^{*2} 4p$	1	${}^3D_1^o$	821639	822168
8	$4s 4p^2 4p^*$	2	${}^3D_2^o$	939867	949269
9	$4s 4p^2 4p^*$	3	${}^3D_3^o$	997814	999419
10	$4s 4p^2 4p^*$	0	${}^3P_0^o$	1035369	1035099
11	$4s 4p^2 4p^*$	1	${}^3P_1^o$	1060931	1063093
12	$4s^2 4p^* 4d^*$	2	${}^3F_2^o$	1080696	1087372
13	$4s 4p^2 4p^*$	2	${}^1D_2^o$	1087278	1086259
14	$4s 4p^2 4p^*$	1	${}^3S_1^o$	1092968	1095006
15	$4s^2 4p^* 4d^*$	1	${}^3D_1^o$	1162888	1164692
16	$4s^2 4p^* 4d$	3	${}^3F_3^o$	1177511	1179638
17	$4s^2 4p^* 4d$	2	${}^3D_2^o$	1180541	1181319
18	$4s 4p^3$	2	${}^3P_2^o$	1275469	1276306
19	$4s 4p^3$	1	${}^1P_1^o$	1357027	1359381
20	$4s^2 4p 4d^*$	2	${}^1D_2^o$	1365276	1368743
21	$4s^2 4p 4d$	4	${}^3F_4^o$	1377169	1385402
22	$4s^2 4p 4d^*$	0	${}^3P_0^o$	1385658	1386850
23	$4s^2 4p 4d^*$	1	${}^3P_1^o$	1389923	1392882
24	$4s^2 4p 4d^*$	3	${}^3D_3^o$	1396066	1395207
25	$4s^2 4p 4d$	2	${}^3P_2^o$	1423644	1425000
26	$4s^2 4p 4d$	3	${}^1F_3^o$	1489096	1489851
27	$4s^2 4p 4d$	1	${}^1P_1^o$	1496468	1497342
28	$4p^{*2} 4p^2$	2	${}^3P_2^e$	1620136	1629921
29	$4p^{*2} 4p^2$	0	${}^1S_0^e$	1668309	1674826
30	$4p^* 4p^3$	1	${}^3P_1^e$	1855288	1869582
31	$4p^* 4p^3$	2	${}^1D_2^e$	1886205	1894431
32	$4p^4$	0	${}^3P_0^e$	2142074	2153497

Table (3): **MCDF** and **HFR** energy levels (in cm^{-1}) of $4s^24p^2$, $4s4p^3$, $4s^24p4d$, and $4p^4$ configurations for Pm XXX ion.

	JJ-coupling	J	LS	MCDF (cm^{-1})	HFR (cm^{-1})
1	$4s^2 4p^{*2}$	0	${}^3P_0^e$	0	0
2	$4s^2 4p^* 4p$	1	${}^3P_1^e$	249494	248488
3	$4s^2 4p^* 4p$	2	${}^1D_2^e$	275841	271768
4	$4s^2 4p^2$	2	${}^3P_2^e$	539901	537630
5	$4s^2 4p^2$	0	${}^1S_0^e$	589970	588496
6	$4s 4p^{*2} 4p$	2	${}^5S_2^o$	769570	775523
7	$4s 4p^{*2} 4p$	1	${}^3D_1^o$	865227	866784
8	$4s 4p^2 4p^*$	2	${}^3D_2^o$	1007307	1013638
9	$4s 4p^2 4p^*$	3	${}^3D_3^o$	1067977	1065797
10	$4s 4p^2 4p^*$	0	${}^3P_0^o$	1106584	1102389
11	$4s 4p^2 4p^*$	1	${}^3P_1^o$	1132493	1131951
12	$4s^2 4p^* 4d^*$	2	${}^3F_2^o$	1134604	1138348
13	$4s 4p^2 4p^*$	2	${}^1D_2^o$	1158199	1155412
14	$4s 4p^2 4p^*$	1	${}^3S_1^o$	1164650	1162721
15	$4s^2 4p^* 4d^*$	1	${}^3D_1^o$	1217771	1217851
16	$4s^2 4p^* 4d$	2	${}^3D_2^o$	1238708	1238807
17	$4s^2 4p^* 4d$	3	${}^3F_3^o$	1238924	1237952
18	$4s 4p^3$	2	${}^3P_2^o$	1368887	1366796
19	$4s^2 4p 4d^*$	2	${}^1D_2^o$	1445988	1445639
20	$4s 4p^3$	1	${}^1P_1^o$	1453266	1452404
21	$4s^2 4p 4d^*$	0	${}^3P_0^o$	1461020	1463923
22	$4s^2 4p 4d$	4	${}^3F_4^o$	1461690	1466448
23	$4s^2 4p 4d^*$	1	${}^3P_1^o$	1470934	1470238
24	$4s^2 4p 4d^*$	3	${}^3D_3^o$	1470993	1472577
25	$4s^2 4p 4d$	2	${}^3P_2^o$	1508700	1506544
26	$4s^2 4p 4d$	3	${}^1F_3^o$	1575274	1572440
27	$4s^2 4p 4d$	1	${}^1P_1^o$	1583765	1580874
28	$4p^{*2} 4p^2$	2	${}^3P_2^e$	1711287	1716606
29	$4p^{*2} 4p^2$	0	${}^1S_0^e$	1760973	1762856
30	$4p^* 4p^3$	1	${}^3P_1^e$	1970057	1980763
31	$4p^* 4p^3$	2	${}^1D_2^e$	2001639	2006177
32	$4p^4$	0	${}^3P_0^e$	2281604	2290109

Table (4): **MCDF** and **HFR** energy levels (in cm^{-1}) of $4s^24p^2$, $4s4p^3$, $4s^24p4d$, and $4p^4$ configurations for Sm XXXI ion.

	JJ-coupling	J	LS	MCDF (cm^{-1})	HFR (cm^{-1})
1	$4s^2 4p^{*2}$	0	${}^3P_0^e$	0	0
2	$4s^2 4p^* 4p$	1	${}^3P_1^e$	274985	274369
3	$4s^2 4p^* 4p$	2	${}^1D_2^e$	300258	298308
4	$4s^2 4p^2$	2	${}^3P_2^e$	591556	590529
5	$4s^2 4p^2$	0	${}^1S_0^e$	642768	642538
6	$4s 4p^{*2} 4p$	2	${}^5S_2^o$	815001	820156
7	$4s 4p^{*2} 4p$	1	${}^3D_1^o$	912576	913375
8	$4s 4p^2 4p^*$	2	${}^3D_2^o$	1074337	1081955
9	$4s 4p^2 4p^*$	3	${}^3D_3^o$	1129853	1136067
10	$4s 4p^2 4p^*$	0	${}^3P_0^o$	1177304	1173571
11	$4s^2 4p^* 4d^*$	2	${}^3F_2^o$	1187477	1191061
12	$4s 4p^2 4p^*$	1	${}^3P_1^o$	1204821	1204693
13	$4s 4p^2 4p^*$	2	${}^1D_2^o$	1230972	1228406
14	$4s 4p^2 4p^*$	1	${}^3S_1^o$	1235868	1234354
15	$4s^2 4p^* 4d^*$	1	${}^3D_1^o$	1273388	1272739
16	$4s^2 4p^* 4d$	3	${}^3F_3^o$	1299914	1298395
17	$4s^2 4p^* 4d$	2	${}^3D_2^o$	1304232	1298424
18	$4s 4p^3$	2	${}^3P_2^o$	1463609	1463125
19	$4s^2 4p 4d^*$	2	${}^1D_2^o$	1506402	1526162
20	$4s^2 4p 4d^*$	0	${}^3P_0^o$	1542543	1544624
21	$4s^2 4p 4d$	4	${}^3F_4^o$	1545983	1551524
22	$4s 4p^3$	1	${}^1P_1^o$	1550772	1551224
23	$4s^2 4p 4d^*$	1	${}^3P_1^o$	1551523	1551226
24	$4s^2 4p 4d^*$	3	${}^3D_3^o$	1551599	1553577
25	$4s^2 4p 4d$	2	${}^3P_2^o$	1578874	1592126
26	$4s^2 4p 4d$	3	${}^1F_3^o$	1662685	1659057
27	$4s^2 4p 4d$	1	${}^1P_1^o$	1671326	1668433
28	$4p^{*2} 4p^2$	2	${}^3P_2^e$	1802109	1807270
29	$4p^{*2} 4p^2$	0	${}^1S_0^e$	1853301	1854856
30	$4p^* 4p^3$	1	${}^3P_1^e$	2086241	2097815
31	$4p^* 4p^3$	2	${}^1D_2^e$	2118487	2123796
32	$4p^4$	0	${}^3P_0^e$	2424302	2434492

Table (5): **MCDF** and **HFR** energy levels (in cm^{-1}) of $4s^24p^2$, $4s4p^3$, $4s^24p4d$, and $4p^4$ configurations for **Eu XXXII** ion.

	JJ-coupling	J	LS	MCDF (cm^{-1})	HFR (cm^{-1})
1	$4s^2 4p^{*2}$	0	${}^3P_0^e$	0	0
2	$4s^2 4p^* 4p$	1	${}^3P_1^e$	301522	302192
3	$4s^2 4p^* 4p$	2	${}^1D_2^e$	327601	326786
4	$4s^2 4p^2$	2	${}^3P_2^e$	646099	647308
5	$4s^2 4p^2$	0	${}^1S_0^e$	698460	700465
6	$4s 4p^{*2} 4p$	2	${}^5S_2^o$	848063	866736
7	$4s 4p^{*2} 4p$	1	${}^3D_1^o$	959882	961948
8	$4s 4p^2 4p^*$	2	${}^3D_2^o$	1144514	1154272
9	$4s 4p^2 4p^*$	3	${}^3D_3^o$	1202520	1210284
10	$4s^2 4p^* 4d^*$	2	${}^3F_2^o$	1241426	1245740
11	$4s 4p^2 4p^*$	0	${}^3P_0^o$	1252957	1248700
12	$4s 4p^2 4p^*$	1	${}^3P_1^o$	1280227	1281373
13	$4s 4p^2 4p^*$	2	${}^1D_2^o$	1306780	1305303
14	$4s 4p^2 4p^*$	1	${}^3S_1^o$	1310344	1309965
15	$4s^2 4p^* 4d^*$	1	${}^3D_1^o$	1330091	1329585
16	$4s^2 4p^* 4d$	2	${}^3D_2^o$	1352210	1360416
17	$4s^2 4p^* 4d$	3	${}^3F_3^o$	1362383	1361208
18	$4s 4p^3$	2	${}^3P_2^o$	1563290	1565394
19	$4s^2 4p 4d^*$	2	${}^1D_2^o$	1591064	1610584
20	$4s^2 4p 4d^*$	0	${}^3P_0^o$	1625781	1629229
21	$4s^2 4p 4d$	4	${}^3F_4^o$	1632600	1640921
22	$4s^2 4p 4d^*$	1	${}^3P_1^o$	1635036	1636119
23	$4s^2 4p 4d^*$	3	${}^3D_3^o$	1635131	1638483
24	$4s 4p^3$	1	${}^1P_1^o$	1653206	1655947
25	$4s^2 4p 4d$	2	${}^3P_2^o$	1666883	1682038
26	$4s^2 4p 4d$	3	${}^1F_3^o$	1751952	1750000
27	$4s^2 4p 4d$	1	${}^1P_1^o$	1761715	1760312
28	$4p^{*2} 4p^2$	2	${}^3P_2^e$	1896199	1901961
29	$4p^{*2} 4p^2$	0	${}^1S_0^e$	1948890	1950876
30	$4p^* 4p^3$	1	${}^3P_1^e$	2207530	2220831
31	$4p^* 4p^3$	2	${}^1D_2^e$	2240442	2247383
32	$4p^4$	0	${}^3P_0^e$	2573953	2586788

Table (11): Continued.

Z	Initial	Final	MCDF		HFR	
			A_L (sec⁻¹)	f_L	A_L (sec⁻¹)	f_L
62	$4s^2 4p^2 {}^3P_0^e$	$4s 4p^3 {}^3D_1^o$	1.624E+11	8.878E-01	1.808E+11	9.750E-01
	$4s^2 4p^2 {}^3P_1^e$	$4s 4p^3 {}^3S_1^o$	8.171E+10	1.342E-01	9.150E+10	1.489E-01
	$4s^2 4p^2 {}^3P_1^e$	$4s 4p^3 {}^3P_1^o$	2.257E+11	3.961E-01	1.995E+11	3.458E-01
	$4s^2 4p^2 {}^3P_2^e$	$4s 4p^3 {}^3D_3^o$	1.613E+10	1.193E-01	1.829E+10	1.288E-01
	$4s^2 4p^2 {}^3P_2^e$	$4s 4p^3 {}^3P_2^o$	1.744E+11	3.483E-01	1.727E+11	3.396E-01
	$4s^2 4p^2 {}^3P_2^e$	$4s 4p^3 {}^1P_1^o$	3.061E+11	3.028E-01	3.146E+11	3.069E-01
	$4s^2 4p^2 {}^3P_0^e$	$4s^2 4p 4d {}^3D_1^o$	4.645E+11	1.289E+00	5.153E+11	1.432E+00
	$4s^2 4p^2 {}^1D_2^e$	$4s^2 4p 4d {}^1F_3^o$	1.226E+11	1.386E-01	9.926E+10	1.125E-01
	$4s^2 4p^2 {}^1D_2^e$	$4s^2 4p 4d {}^3F_3^o$	1.104E+11	2.320E-01	1.287E+11	2.698E-01
	$4s^2 4p^2 {}^3P_2^e$	$4s^2 4p 4d {}^3P_2^o$	1.744E+11	3.483E-01	1.727E+11	3.396E-01
	$4s^2 4p^2 {}^3P_2^e$	$4s^2 4p 4d {}^1F_3^o$	4.342E+11	7.946E-01	4.491E+11	8.261E-01
	$4s 4p^3 {}^3P_0^0$	$4p^4 {}^3P_1^e$	4.317E+10	2.379E-01	4.870E+10	2.564E-01
	$4s 4p^3 {}^3P_1^0$	$4p^4 {}^3P_2^e$	1.107E+10	7.902E-02	9.346E+09	6.425E-02
	$4s 4p^3 {}^1D_2^0$	$4p^4 {}^1D_2^e$	1.479E+11	2.851E-01	1.921E+11	3.589E-01
	$4s 4p^3 {}^3D_1^0$	$4p^4 {}^3P_2^e$	8.339E+10	2.666E-01	9.874E+10	3.089E-01
	$4s 4p^3 {}^3D_1^0$	$4p^4 {}^1S_0^e$	1.600E+11	9.142E-02	2.179E+11	1.230E-01
	$4s 4p^3 {}^3S_1^0$	$4p^4 {}^3P_2^e$	1.261E+10	1.002E-01	1.545E+10	1.177E-01
	$4s 4p^3 {}^1P_1^0$	$4p^4 {}^1D_2^e$	2.206E+10	1.744E-01	2.522E+10	1.923E-01
63	$4s^2 4p^2 {}^3P_0^e$	$4s 4p^3 {}^3D_1^o$	1.813E+11	8.962E-01	8.962E-01	8.962E-01
	$4s^2 4p^2 {}^3P_1^e$	$4s 4p^3 {}^3S_1^o$	8.784E+10	1.310E-01	9.867E+10	1.455E-01
	$4s^2 4p^2 {}^3P_1^e$	$4s 4p^3 {}^3P_1^o$	2.535E+11	4.017E-01	2.234E+11	3.490E-01
	$4s^2 4p^2 {}^3P_2^e$	$4s 4p^3 {}^3D_3^o$	1.706E+10	1.182E-01	1.926E+10	1.277E-01
	$4s^2 4p^2 {}^3P_2^e$	$4s 4p^3 {}^3P_2^o$	1.894E+11	3.421E-01	1.878E+11	3.342E-01
	$4s^2 4p^2 {}^3P_2^e$	$4s 4p^3 {}^1P_1^o$	3.359E+11	3.015E-01	3.450E+11	3.048E-01
	$4s^2 4p^2 {}^3P_0^e$	$4s^2 4p 4d {}^3D_1^o$	5.035E+11	1.281E+00	5.583E+11	1.419E+00
	$4s^2 4p^2 {}^1D_2^e$	$4s^2 4p 4d {}^1F_3^o$	1.227E+11	1.270E-01	9.823E+10	1.019E-01
	$4s^2 4p^2 {}^1D_2^e$	$4s^2 4p 4d {}^3F_3^o$	1.217E+11	2.387E-01	1.405E+11	2.754E-01
	$4s^2 4p^2 {}^3P_2^e$	$4s^2 4p 4d {}^3P_2^o$	1.664E+11	2.396E-01	1.894E+11	2.655E-01
	$4s^2 4p^2 {}^3P_2^e$	$4s^2 4p 4d {}^1F_3^o$	4.568E+11	7.843E-01	4.711E+11	8.129E-01
	$4s 4p^3 {}^3P_0^0$	$4p^4 {}^3P_1^e$	4.981E+10	2.490E-01	5.393E+10	2.564E-01
	$4s 4p^3 {}^3P_1^0$	$4p^4 {}^3P_2^e$	1.154E+10	7.751E-02	9.690E+09	6.293E-02
	$4s 4p^3 {}^1D_2^0$	$4p^4 {}^1D_2^e$	1.689E+11	2.943E-01	2.180E+11	3.682E-01
	$4s 4p^3 {}^3D_1^0$	$4p^4 {}^3P_2^e$	9.512E+10	2.746E-01	1.118E+11	3.161E-01
	$4s 4p^3 {}^3D_1^0$	$4p^4 {}^1S_0^e$	1.822E+11	9.422E-02	2.463E+11	1.259E-01
	$4s 4p^3 {}^3S_1^0$	$4p^4 {}^3P_2^e$	1.311E+10	9.587E-02	1.561E+10	1.114E-01
	$4s 4p^3 {}^1P_1^0$	$4p^4 {}^1D_2^e$	2.283E+10	1.688E-01	2.602E+10	1.862E-01

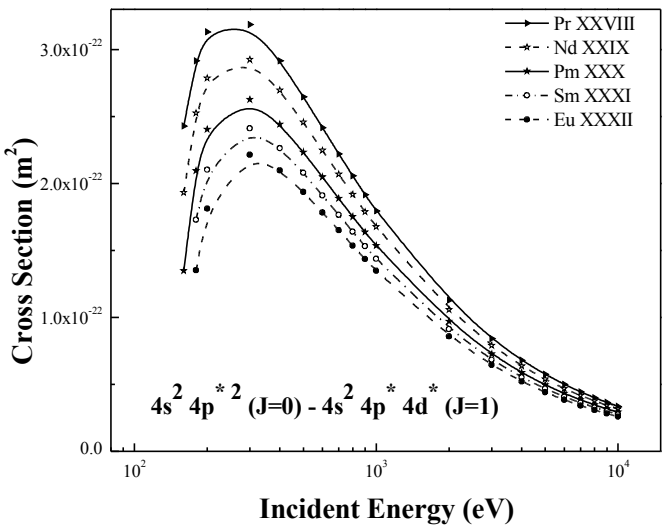


Fig. 1:
The behavior of cross section (m^2)
of
 $4s^2 4p^{*2} (J=0) - 4s^2 4p^* 4d^* (J=1)$
for Ge-like ions

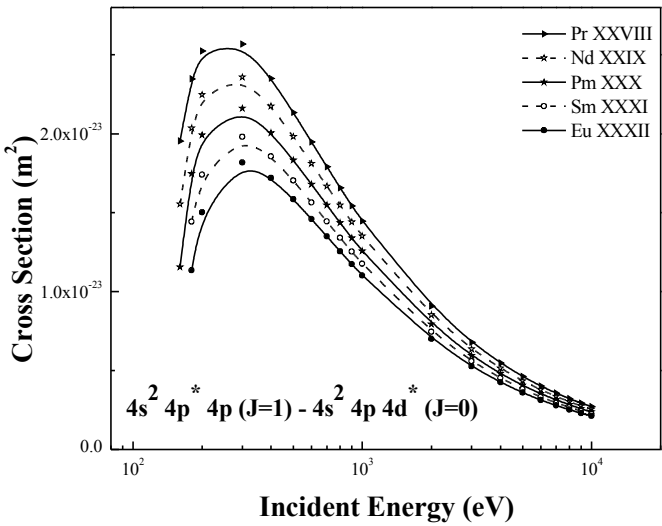


Fig. 2:
The behavior of cross section (m^2)
of
 $4s^2 4p^* 4p (J=1) - 4s^2 4p 4d^* (J=0)$
for Ge-like ions.

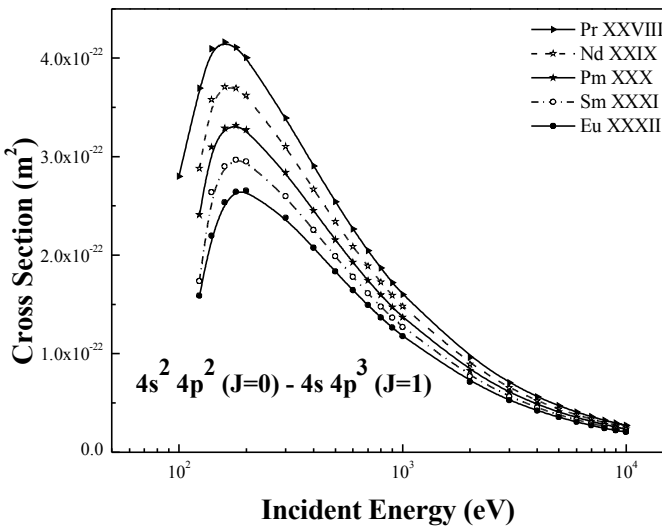


Fig. 3:
The behavior of cross section (m^2)
of
 $4s^2 4p^2 (J=0) - 4s 4p^3 (J=1)$
for Ge-like ions.

